

采用人工表面等离子激元电极的慢光铌酸锂电光调制器

徐光耀, 马晓飞, 盛冲, 刘辉*

南京大学物理学院固体微结构物理国家重点实验室, 人工微结构科学与技术协同中心, 江苏 南京 210093

摘要 高速率、低功耗的小型化电光调制器是现代电通信网络和微波光子系统的关键组成部分。基于人工表面等离子激元的慢光效应,设计了一种利用金属光子晶体电极的马赫-曾德尔干涉仪电光调制器。通过在薄膜铌酸锂光子芯片上调控微波色散与群速度,实现了微波与光波之间更强的相互耦合作用。对电光重叠积分因子的分析表明,这种结构相较于条形电极结构可以通过更短的传播长度得到相同的相移,实现高效的调制过程。同时,所提慢光效应结构也可以应用于其他集成化的电光器件。

关键词 光学器件; 电光调制器; 人工表面等离子激元; 慢光效应; 薄膜铌酸锂

中图分类号 O436 文献标志码 A

DOI: 10.3788/AOS230790

1 引言

由于现代社会计算机网络与多媒体技术的进步,数据通信的业务流量呈现指数型增长,这种快速扩展对所有层级光网络中的收发器提出了严峻的挑战,即如何在显著提高数据速率的同时,降低功耗与成本。电光调制器可以将高速的电信号编码转换到光信号中,是现代光通信链路的核心部分。人们为实现高性能的电光调制器在各类材料平台上^[1-9]作出了巨大的努力,其中,硅上绝缘体(SOI)平台的硅光子学技术^[1-2]由于能在互补金属氧化物半导体(CMOS)铸造厂以低成本大批量地生产光子集成电路被认为是较优选择,然而硅中的调制主要依赖于自由载流子的色散效应,其本质是存在吸收与非线性的,因此降低了光调制幅度。其他基于 III-V 族^[3]以及聚合物^[4]等材料的平台,由于材料的内在限制,无法实现兼容 CMOS 电压的超高电光带宽与极低光学损耗的电光调制器。

铌酸锂(LiNbO₃)由于其优异的电光特性而成为电光调制器的首选材料,但大多数商用 LiNbO₃调制器仍然基于传统的钛扩散与质子交换波导^[10-11],这些波导具有较低的折射率对比度,核心与包层的折射率差仅约为 0.02,导致光学模式尺寸较大,这种弱光约束要求电极放在远离光波导的位置,调制效率较低。近年来,绝缘体上铌酸锂(LNOI)薄膜波导器件^[12-14]由于具有高折射率对比度,能够实现对光场的强约束与低

损耗,研究人员已经在此平台上实现了许多兼具低电压与大带宽的电光调制器^[14-17]以及宽带非线性器件^[18],并通过灵活设计电光调制器的电极结构^[19-21],大幅降低了射频损耗,使得电光带宽超过 100 GHz。同样有许多研究针对光波导的空间结构进行设计^[22-24],优化光波的传输与色散特性,实现了更紧凑与小型化的器件。目前人们仍在寻求各种方式,期望在实现较大电光带宽的同时,使得器件的调制效率同样处于较高水平。

近年来,人们对于在微波波段利用人工表面等离子激元^[25-27]和光子晶体^[28]等金属超材料操控电磁波的兴趣越来越浓厚,因其亚波长的结构可以将微波电场束缚在较小尺寸内,相应空间内的电场可以实现极大的压缩与增强。若能在金属电极之间的间距保持不变的情况下,使得 LiNbO₃波导内的调制微波电场增强,增大波导内微波与光波模式的耦合强度,则在施加相同电压时,可以使 LiNbO₃波导内的光波获得更大的相移,提高电光调制效率。目前关于将具有人工表面等离子激元微结构的金属电极与 LiNbO₃波导异质集成设计电光调制器的研究还几乎没有。

本文通过研究人工表面等离子激元电极色散以及慢光效应,设计了一种利用锯齿形金属光子晶体电极的单片异质集成薄膜 LiNbO₃马赫-曾德尔干涉仪(MZI)电光调制器。通过调控微波模式的色散曲线实现光波与微波速度匹配的同时,利用金属光子晶体在带边位

收稿日期: 2023-04-10; 修回日期: 2023-05-05; 录用日期: 2023-05-10; 网络首发日期: 2023-05-20

基金项目: 国家自然科学基金(92163216, 92150302, 62288101)

通信作者: *liuhui@nju.edu.cn

置较强的慢光效应,使局域在亚波长金属齿中的微波模场大幅增强,提高光波与微波之间的相互耦合作用与重叠体积,使得薄膜 LiNbO₃ 波导内发生的电光效应更加强烈。微波群速度与电光重叠积分因子表明,与无周期单元结构的直波导调制器相比,利用金属光子晶体电极的结构在 MZI 调制器的一条臂上改变相同相位 π 时,具有更短的器件长度,在满足器件趋向小型化便于集成的同时,减少了器件的总损耗值,增大了电光带宽,真正实现了兼顾低电压与大带宽的小型集成化调制器件。

2 样品设计与模拟分析

图 1 为利用人工表面等离子激元电极设计的薄膜 LiNbO₃ 电光调制器的示意图。图 1(b) 为电光调制器的俯视示意图,入射光通过 Y 结分为相同的两束进入 LiNbO₃ 波导,即 MZI 调制器的两条臂中,两波导位于共面微波传输带线的电极间隙中,在外加微波场的作用下,通过线性电光效应使 LiNbO₃ 波导的模式有效折射率发生改变,由于外加电场在两条臂上的方向相反,其中,一条臂发生光学相位推进,而另一条发生相位延迟,在输出端的 Y 结处由于存在相位差,两束光发生干涉作用,即可以实现对输出信号光振幅的调制。图 1(c) 展示了器件的截面结构,在厚度 h_{Si} 为 500 μm 的 Si

衬底上沉积厚 $h_{\text{SiO}_2, \text{buffer}}$ 为 4.7 μm 的 SiO₂ 缓冲层,微波模式的电场主要驻留在其中,在缓冲层上方将厚度 h_1 为 600 nm 的 x 切 LiNbO₃ 薄膜刻穿使其顶部宽度 w_0 为 1 μm 、波导倾角为 70°。

人工表面等离子激元金属电极则置于波导两侧,其电场的主分量与 LiNbO₃ 晶面的 z 轴平行,可以最大程度地利用电光系数 γ_{33} 。电极为周期性结构,其形状包括齿部分与槽部分,具体参数如下:电极主体宽度 $w_1 = w_2 = 20 \mu\text{m}$,电极厚度 $h_2 = 0.8 \mu\text{m}$,周期 $p = p_1 + p_2 = 250 \mu\text{m}$,其中, $p_1 = p_2 = 125 \mu\text{m}$,金属锯齿宽度 $d = 8 \mu\text{m}$ 。金属电极越靠近 LiNbO₃ 波导,对光波的吸收损耗越大,这限制了微波场与光波场的交叠程度,而刻穿的 LiNbO₃ 波导可以将光波更好地约束在其中,减少倏逝波的衰减区域,这样可以将金属电极的间距减小而保持金属对光波的低吸收损耗。图 2(a) 展示了光波吸收损耗随电极间距的变化,当间距小于 3 μm 时,吸收损耗急剧增大,因此在保证损耗尽量小的同时,使得电光重叠最大,将电极间距 g 设定为 3 μm ,最后在器件上方覆盖厚度 $h_{\text{SiO}_2, \text{cladding}}$ 为 2 μm 的 SiO₂ 保护层。由于齿与槽部分可单独分别等效为不同有效折射率的介质,因此它们按照周期性排列起来的结构可认为是一维光子晶体,整个器件同样兼具光子晶体的特性。

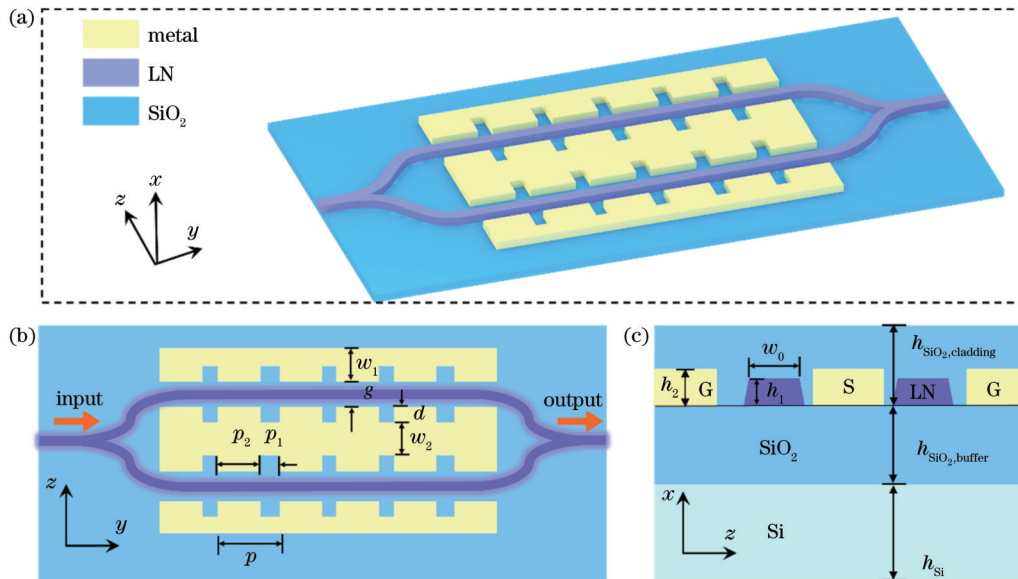


图 1 薄膜 LiNbO₃ 上利用人工表面等离子激元金属电极的 MZI 电光调制器结构。(a) 金属光子晶体电极的 MZI 电光调制器结构;(b) MZI 电光调制器的纵截面结构;(c) MZI 电光调制器的横截面结构

Fig. 1 Structure of thin-film lithium niobate MZI electro-optic modulator with spoof surface plasmon polariton electrodes. (a) Structure of MZI electro-optic modulator with metal photonic crystal electrodes; (b) longitudinal section structure of MZI electro-optic modulator; (c) cross-section structure of MZI electro-optic modulator

使用有限元数值仿真软件——COMSOL MultiPhysics 的波动光学模块分别对电光调制器的光学模式与微波模式进行模场分布与色散曲线计算。微波与光波模式的模场分布如图 2(b) 所示,二者在

LiNbO₃ 波导内相互耦合与交叠,实现高效的电光调制。图 2(c) 为光波的色散曲线,可从中计算频率为 193.5 THz 的光波群折射率,为 2.296,为了使得调制相位能够持续地积累,根据能量与动量守恒关系,应当满足传

输光波的群速度与调制微波的相速度匹配,即使光波群折射率与微波的有效折射率相等。在满足速度匹配

的同时,为了利用微波的慢光效应以增强电光耦合强度,将速度匹配点设计在微波色散曲线的带边处。

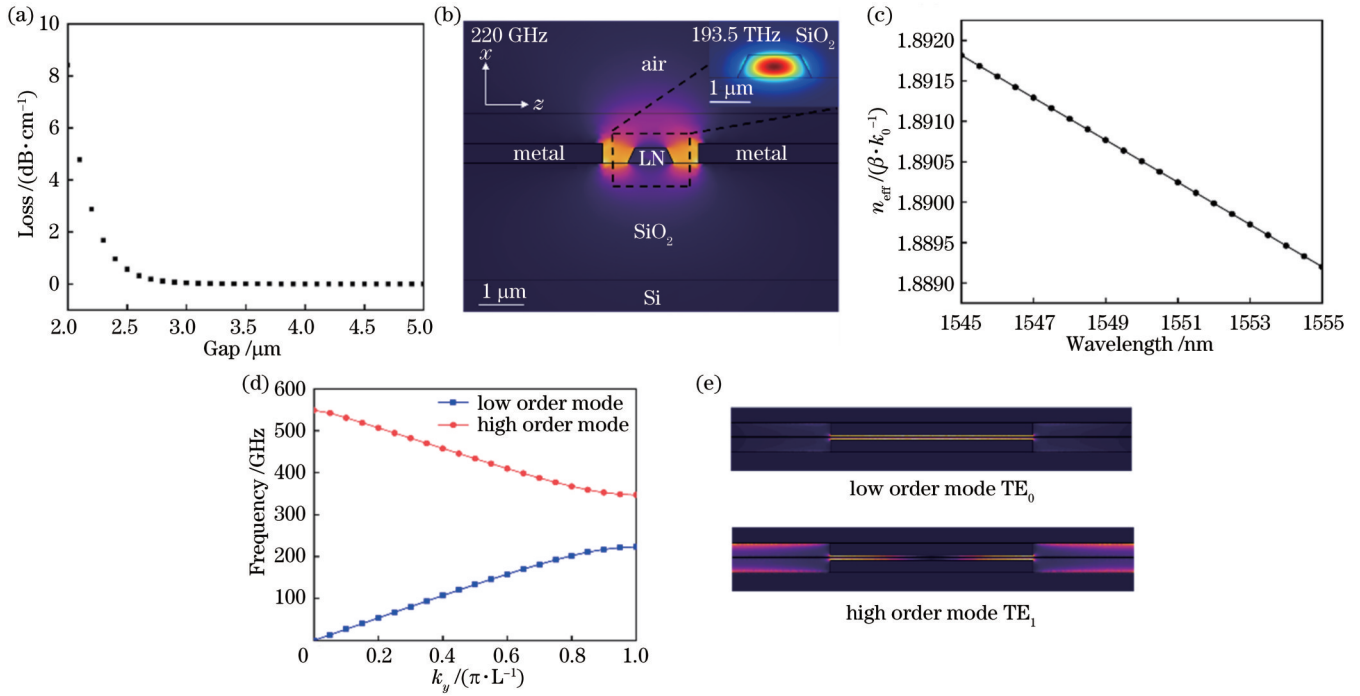


图 2 慢光效应薄膜 LiNbO₃ 电光调制器的电磁特性。(a) 光吸收损耗随电极间距的变化关系;(b) 特征频率 220 GHz 的微波模式 TE₀ 与 193.5 THz 的光波模式 TE₀₀ 的本征模场分布(插图内);(c) LiNbO₃ 电光调制器光波模式 TE₀₀ 的色散曲线;(d) LiNbO₃ 电光调制器的微波模式 TE₀ 与 TE₁ 色散曲线;(e) 金属光子晶体结构单元的微波本征模场 TE₀ 与 TE₁ 纵截面分布

Fig. 2 Electromagnetic characteristics of slow light effect thin-film lithium niobate electro-optic modulators. (a) Variation of optical loss with the gap of electrodes; (b) eigenmode field distributions of microwave mode TE₀ with a eigenfrequency of 220 GHz and light wave mode TE₀₀ with a frequency of 193.5 THz (as shown in the inset); (c) dispersion curve of light wave mode TE₀₀ of lithium niobate electro-optic modulators; (d) dispersion curves of microwave modes TE₀ and TE₁ of lithium niobate electro-optic modulators; (e) longitudinal section of microwave eigenmodes field distributions TE₀ and TE₁ of metal photonic crystal unit

从图 2(d) 可以看出,由于光子晶体的特性,微波色散曲线的频率值逐渐趋于平缓,并在带边处形成带隙,且在逐渐靠近带边时,微波模式 TE₀ 的有效折射率值也逐渐增大,因此可以根据需求灵活调控金属光子晶体的几何参数,实现完美速度匹配,而避免单一地调控 SiO₂ 缓冲层的厚度。图 2(e) 则展示了周期单元内两种微波模场沿传播方向 y 的分布,低阶模式 TE₀ 模场主要局域在有效折射率较大的金属齿部分,且中间位置的场最强,而高阶模式 TE₁ 的模场逐渐局域到金属槽部分,中间位置的电场接近 0。

3 理论计算与讨论

对于 x 切薄膜 LiNbO₃ 电光调制器,由于使用的是光波的基模模式 TE₀₀,其偏振方向平行于 LiNbO₃ 晶体光轴 z 轴,在这种情况下,波导的折射率变化仅受到调制微波电场的 z 分量影响,而参与导模有效折射率变化的调制电场比例取决于电场 z 方向分量与光场在空间上的重叠状态,导模有效折射率的改变量为

$$\Delta n_{\text{eff}} = \frac{1}{2} \Gamma \gamma_{33} n_e^3 |\overline{E_z}|, \quad (1)$$

$$\Gamma = \frac{G}{V} \frac{\iint |E_o(x, z)|^2 E_{r,z}(x, z) dx dz}{\iint |E_o(x, z)|^2 dx dz}, \quad (2)$$

式中: γ_{33} 为 LiNbO₃ 晶体在 z 方向偏振光下的电光系数; n_e 为 LiNbO₃ 晶体的非常光折射率; $|\overline{E_z}|$ 为整个几何空间的微波电场 z 分量的平均值,其大小可以近似表示为 V/G ; Γ 为电光重叠积分因子; G 为一条波导臂两侧电极之间的间距; V 为施加在信号极上的电压; $|E_o(x, z)|$ 为 LiNbO₃ 波导内的光波电场模; $E_{r,z}(x, z)$ 为 LiNbO₃ 波导内沿方向 z 的微波电场分量,下标 o 与 r 为电磁波的种类,分别代表光波与微波,下标 z 代表沿 z 方向的分量。对于使用无周期结构的条形电极的 LiNbO₃ 电光调制器,由于微波电场在传播方向 y 上的每个位置都相同,因此可以利用上述公式计算。但对于利用有周期结构的金属光子晶体电极的电光调制器,由于其微波电场在传播方向 y 上分布不均,因此需要在整个三维空间中重新定义其导模有效折射率变化量对线性电光效应的响应,电光重叠积分因子可改写为

$$\Gamma = \frac{G}{V} \frac{\iiint |E_o(x, z)|^2 E_{rf,z}(x, y, z) dx dy dz}{\iiint |E_o(x, z)|^2 dx dy dz}. \quad (3)$$

因此,电光效应导致的相移改变量为

$$\Delta\varphi = \Delta\beta L = \Delta n_{\text{eff}} k_0 L =$$

$$n_e^3 \gamma_{33} \frac{\pi L}{\lambda_0} \frac{\iiint |E_o(x, z)|^2 E_{rf,z}(x, y, z) dx dy dz}{\iiint |E_o(x, z)|^2 dx dy dz}, \quad (4)$$

式中: $\Delta\varphi$ 为电光效应导致的相移量; $\Delta\beta$ 为光波传播常数的改变量; L 为传播长度; k_0 为被调制的光波在真空中的波矢大小; λ_0 为被调制的光波在真空中的波长,下标0代表电磁波在真空中的相关信息。

为了探究调制微波的慢光效应对于LiNbO₃波导的

线性电光效应强度大小影响程度,需要合理地对不同结构参数的器件进行对比,定义 $G=g+d$,保持 G 的大小不变,通过改变单一参数 d 的大小,对比不同 d 的器件结构所展示的物理效应。 $G=11\ \mu\text{m}$ 保持不变,将 d 从0变化到 $8\ \mu\text{m}$,其色散关系如图3(a)所示。可以看出, $d=0$ 时对应的是无周期结构单元的直电极,由于其不具备光子晶体的特性,色散曲线趋于线性,不会在带边的位置发生频率的渐近并产生带隙,但随着 d 的增大,色散曲线开始压得更低且带隙逐渐变大。为了进一步探究慢光效应,在色散曲线上取相同的频率 $f=220\ \text{GHz}$,对比不同参数 d 对应的群速度大小,具体如图3(b)所示。 d 增大时对应的群速度先缓慢后急剧减小,由此可见,金属锯齿宽度较大的结构对应的慢光效应越强。

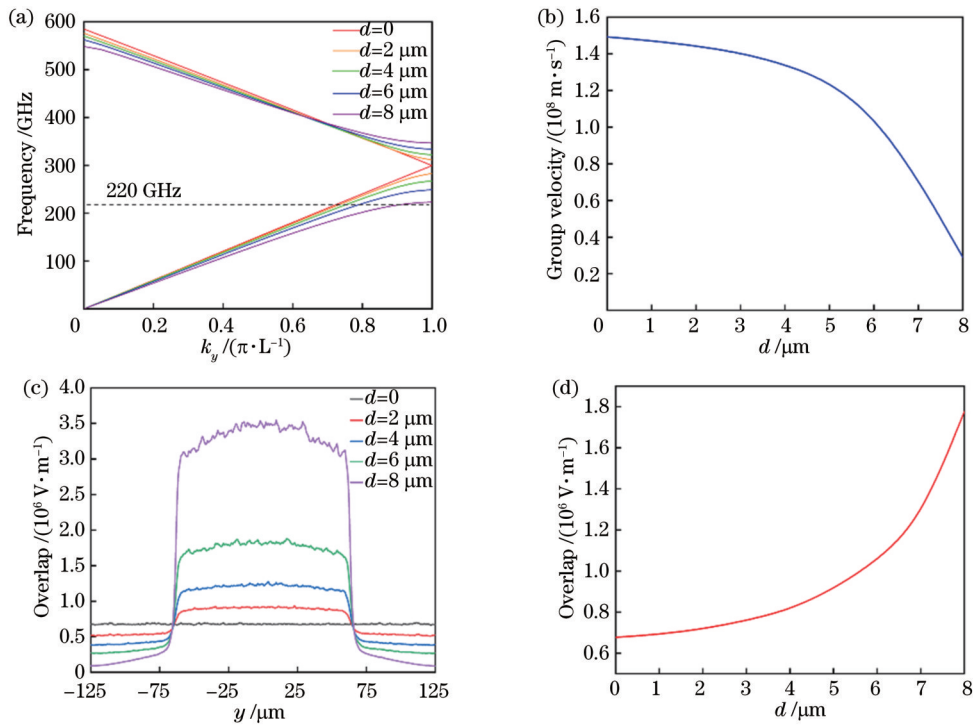


图3 慢光效应电光调制器的调制效果分析。(a)单一参数 d 变化时对应的微波模式色散曲线;(b)相同频率220 GHz时,微波群速度 v_g 随参数 d 的变化关系;(c)周期结构单元内,不同参数 d 对应的电光重叠面积积分因子随传播方向 y 的变化关系;(d)相同频率220 GHz时,电光重叠体积积分因子随参数 d 的变化关系

Fig. 3 Analysis of modulation effect of the slow light effect electro-optic modulators. (a) Dispersion curves of microwave modes with single parameter d changing; (b) variation of group velocity v_g of microwave with parameter d at the same frequency 220 GHz; (c) variation of electro-optic overlap surface integration factor with the propagation direction y of different parameter d of periodic structure unit; (d) variation of electro-optic overlap volume integration factor with parameter d at the same frequency 220 GHz

在发生线性电光效应的LiNbO₃波导内部,慢光效应越强带来的调制微波场增强与局域效果越明显,在图3(c)中,单个周期性元胞内沿传播方向 y 不同位置处的电光重叠程度为

$$\frac{\iint |E_o(x, z)|^2 E_{rf,z}(x, y, z) dx dz}{\iint |E_o(x, z)|^2 dx dz},$$

随着 d 的增大,慢光效应增强,微波电场更加局域在金属齿的部分,槽部分的电场交叠程度则逐渐减弱。而在整个三维空间中,由于沿传播方向 y 上的微波电场

分布不均,电光交叠需要通过计算体积分因子得到,在图3(d)中,纵轴大小为

$$\frac{\iiint |E_o(x, z)|^2 E_{rf,z}(x, y, z) dx dy dz}{\iiint |E_o(x, z)|^2 dx dy dz},$$

代表LiNbO₃波导内的电光耦合作用强度。且随着 d 的增大,调制效果更加明显,具体体现在当实现相同的相移量时,对于 d 越大的结构,所需要的传播长度越短,因此调制效率高,且更利于器件的小型集成化。

4 结 论

人工等离激元结构的慢光效应为薄膜铌酸锂光电调制器芯片提高调制效率提供了新的思路与方法,通过调控人工等离激元结构的几何参数可以灵活设计色散边带位置的微波群速度,并将其限制在亚波长尺度,实现模场的增强与局域,进而大幅增强电光的重叠体积与相互耦合作用。将具有周期结构的金属光子晶体作为电极,并沿铌酸锂光波导传输方向组成共面传输线结构,从而在满足微波与光波速度匹配的条件下,使得电光调制过程能够持续、相干地进行。

根据速度匹配条件,在微波场的色散关系上设计了靠近带边频率处的人工等离激元金属电极,将相应频率的微波场作为调制电场,并进行模拟仿真与计算。用 COMSOL Multiphysics 软件的特征频率模块仿真光波与微波的本征模场分布,计算不同结构下的微波色散曲线与相同频率时慢光的群速度变化曲线,再将相关的电场数据导出计算三维空间中 LiNbO_3 内的电光重叠作用与电光效应,并对同一调制微波频率下不同结构参数的调制结果进行对比。结果表明,随着 z 方向的金属锯齿宽度 d 逐渐增大色散曲线压得越低,群速度越小,因此慢光效应越强,利于增强光与物质的相互作用的同时,也相较无周期结构直电极的调制效果更加优异,并且在实现相同的相移量时,慢光结构的电极可以大幅减小传播长度,对于实现高调制效率与更加紧凑的光子芯片具有重要意义。这种设计思路对于材料平台没有限制,未来也可以应用于其他电光系数较高的材料,更高的调制效率进一步降低了与 CMOS 技术兼容的难度,并且更小的尺寸有利于在同一光子芯片上与其他器件相互集成,以实现功能更复杂与多元化的光子回路。

参 考 文 献

- [1] Streshinsky M, Ding R, Liu Y, et al. Low power 50 Gb/s silicon traveling wave Mach-Zehnder modulator near 1300 nm [J]. *Optics Express*, 2013, 21(25): 30350-30357.
- [2] Azadeh S S, Merget F, Romero-García S, et al. Low $V(\pi)$ Silicon photonics modulators with highly linear epitaxially grown phase shifters[J]. *Optics Express*, 2015, 23(18): 23526-23550.
- [3] Ogiso Y, Ozaki J, Ueda Y, et al. Over 67 GHz bandwidth and 1.5 V $V\pi$ InP-based optical IQ modulator with n-i-p-n heterostructure[J]. *Journal of Lightwave Technology*, 2017, 35(8): 1450-1455.
- [4] Alloatti L, Palmer R, Diebold S, et al. 100 GHz silicon-organic hybrid modulator[J]. *Light: Science & Applications*, 2014, 3(5): e173.
- [5] Haffner C, Heni W, Fedoryshyn Y, et al. All-plasmonic Mach-Zehnder modulator enabling optical high-speed communication at the microscale[J]. *Nature Photonics*, 2015, 9(8): 525-528.
- [6] Mercante A J, Yao P, Shi S Y, et al. 110 GHz CMOS compatible thin film LiNbO_3 modulator on silicon[J]. *Optics Express*, 2016, 24(14): 15590-15595.
- [7] Wang C, Zhang M, Stern B, et al. Nanophotonic lithium niobate electro-optic modulators[J]. *Optics Express*, 2018, 26

- (2): 1547-1555.
- [8] Rao A, Patil A, Rabiei P, et al. High-performance and linear thin-film lithium niobate Mach-Zehnder modulators on silicon up to 50 GHz[J]. *Optics Letters*, 2016, 41(24): 5700-5703.
- [9] Ayata M, Fedoryshyn Y, Heni W, et al. High-speed plasmonic modulator in a single metal layer[J]. *Science*, 2017, 358(6363): 630-632.
- [10] Wooten E L, Kissa K M, Yi-Yan A, et al. A review of lithium niobate modulators for fiber-optic communications systems[J]. *IEEE Journal of Selected Topics in Quantum Electronics*, 2000, 6(1): 69-82.
- [11] Schmidt R V, Kaminow I P. Metal-diffused optical waveguides in LiNbO_3 [J]. *Applied Physics Letters*, 1974, 25(8): 458-460.
- [12] Liang H X, Luo R, He Y, et al. High-quality lithium niobate photonic crystal nanocavities[J]. *Optica*, 2017, 4(10): 1251-1258.
- [13] Zhang M, Wang C, Cheng R, et al. Monolithic ultra-high-Q lithium niobate microring resonator[J]. *Optica*, 2017, 4(12): 1536-1537.
- [14] Wang C, Zhang M, Chen X, et al. Integrated lithium niobate electro-optic modulators operating at CMOS-compatible voltages [J]. *Nature*, 2018, 562(7725): 101-104.
- [15] He M B, Xu M Y, Ren Y X, et al. High-performance hybrid silicon and lithium niobate Mach-Zehnder modulators for 100 Gbit s^{-1} and beyond[J]. *Nature Photonics*, 2019, 13(5): 359-364.
- [16] Xu M Y, He M B, Zhang H G, et al. High-performance coherent optical modulators based on thin-film lithium niobate platform[J]. *Nature Communications*, 2020, 11: 3911.
- [17] Zhang M, Wang C, Kharel P, et al. Integrated lithium niobate electro-optic modulators: when performance meets scalability[J]. *Optica*, 2021, 8(5): 652-667.
- [18] 宗心牧, 黄春雨, 盛冲, 等. 铌酸锂变换光学波导中彩虹捕获与宽带非线性[J]. *光学学报*, 2022, 42(21): 2126012.
Zong X M, Huang C Y, Sheng C, et al. Rainbow capture and broadband nonlinearity in lithium niobate conversion optical waveguide[J]. *Acta Optica Sinica*, 2022, 42(21): 2126012.
- [19] Kharel P, Reimer C, Luke K, et al. Breaking voltage-bandwidth limits in integrated lithium niobate modulators using micro-structured electrodes[J]. *Optica*, 2021, 8(3): 357-363.
- [20] Wang Z, Chen G X, Ruan Z L, et al. Silicon-lithium niobate hybrid intensity and coherent modulators using a periodic capacitively loaded traveling-wave electrode[J]. *ACS Photonics*, 2022, 9(8): 2668-2675.
- [21] Xue Y, Gan R F, Chen K X, et al. Breaking the bandwidth limit of a high-quality-factor ring modulator based on thin-film lithium niobate[J]. *Optica*, 2022, 9(10): 1131-1137.
- [22] Li M X, Ling J W, He Y, et al. Lithium niobate photonic-crystal electro-optic modulator[J]. *Nature Communications*, 2020, 11: 4123.
- [23] Pan B C, Liu H X, Xu H C, et al. Ultra-compact lithium niobate microcavity electro-optic modulator beyond 110 GHz[J]. *Chip*, 2022, 1(4): 100029.
- [24] Huang H J, Han X, Balčytis A, et al. Non-resonant recirculating light phase modulator[J]. *APL Photonics*, 2022, 7(10): 106102.
- [25] Gao X, Zhou L A, Liao Z, et al. An ultra-wideband surface plasmonic filter in microwave frequency[J]. *Applied Physics Letters*, 2014, 104(19): 191603.
- [26] Tang W X, Zhang H C, Ma H F, et al. Concept, theory, design, and applications of spoof surface plasmon polaritons at microwave frequencies[J]. *Advanced Optical Materials*, 2019, 7(1): 1800421.
- [27] Garcia-Vidal F J, Fernández-Domínguez A I, Martín-Moreno L, et al. Spoof surface plasmon photonics[J]. *Reviews of Modern Physics*, 2022, 94(2): 025004.
- [28] Dong J L, Tomasino A, Balistreri G, et al. Versatile metal-wire waveguides for broadband terahertz signal processing and multiplexing[J]. *Nature Communications*, 2022, 13: 741.

Slow-Light Lithium Niobate Electro-Optic Modulators with Spoof Surface Plasmon Polaritons Electrodes

Xu Guangyao, Ma Xiaofei, Sheng Chong, Liu Hui*

Collaborative Innovation Center of Advanced Microstructures, National Laboratory of Solid State Microstructures, School of Physics, Nanjing University, Nanjing 210093, Jiangsu, China

Abstract

Objective Due to the current explosive growth of data traffic, optical transmission systems need to move towards the direction of high speed and low power consumption through modulation. Miniaturized electro-optic modulators are the key components of modern electrical communication networks and microwave-photon systems, which can convert electrical signals into optical domains. Traditional monolithic integrated electro-optic modulators require long electrodes to induce large optical phase shifts and therefore require a trade-off between electro-optic bandwidth and half-wave voltage, which cannot be met with large bandwidth and low voltage simultaneously. To address the above problem, researchers have proposed various solutions with different materials and waveguide structures. However, existing structures are generally weakly bound to the electric fields, and the mutual coupling strength between optical wave and microwave is limited, resulting in low modulation efficiency and large device size. If the modulated microwave can be enhanced to increase the coupling strength between electromagnetic fields in the waveguide, the optical wave can obtain a larger phase shift when the same driving voltage is applied. Therefore, we wish to propose a structure that can dramatically increase the electro-optic overlap volume and coupling strength between optical wave and microwave, so as to improve the electro-optic modulation efficiency and overcome the trade-off between bandwidth and voltage.

Methods In this paper, a model based on the slow-light effect of spoof surface plasmonic polaritons is utilized to obtain a thin-film lithium niobate Mach-Zehnder interferometer electro-optic modulator. Taking advantage of the large electro-optic coefficient of lithium niobate and the characteristics of metal photonic crystal to limit the microwave within the sub-wavelength scale, the electro-optic modulator can significantly enhance efficiency. Moreover, we can flexibly adjust structural parameters to achieve the desired function according to our demands. Specifically, we realize the speed matching condition between optical waves and microwaves at the band edge of the metal photonic crystal by modulating the dispersion relation and group velocity of microwaves on the thin-film lithium niobate photonic chip. The eigenmode field distribution, group velocity, and dispersion relation of optical waves and microwaves are simulated and calculated by the eigenfrequency module of COMSOL Multiphysics software. The structure is then optimized to enhance the slow-light effect at the band edge of the metal photonic crystal. By enhancing the slow-light effect, the microwave mode field can be compressed in the sub-wavelength scale, leading to a significant improvement in the coupling intensity and overlap volume between the optical wave and microwave. This ultimately intensifies the linear electro-optic effect in the thin-film lithium niobate waveguide.

Results and Discussions To demonstrate that the slow-light effect of a metal photonic crystal can improve the modulation efficiency, we calculate the electro-optic overlapping integration factor within lithium niobate waveguide in the three-dimensional space corresponding to structures with different parameters based on the relevant electric field of eigenmodes. Since microwave eigenmode is inhomogeneous in three dimensions, the electro-optic overlapping factor needs to be integrated into a volume. In addition, the modulation results are compared at the same modulated microwave frequency of 220 GHz. Specifically, the result shows that the structure featuring a stronger slow-light effect has a larger electro-optic overlapping integration factor (Fig. 3). Consequently, the proposed device with metal photonic crystal electrodes allows for a shorter propagation length to realize a more efficient modulation process when changing the same phase shift π in one arm of the Mach-Zehnder interferometer compared with the bar electrode structure. As a result, the scheme we proposed not only satisfies the need for miniaturization and integration but also reduces the total loss of the device with a shorter length, which can eventually realize an electro-optic modulator with large bandwidth and low driving voltage.

Conclusions The slow-light effect of the spoof surface plasmonic polaritons structure provides a new idea and method to improve the modulation efficiency of thin-film lithium niobate electro-optic modulator chips. By modulating the structural parameters of the metal photonic crystal electrodes, the speed matching condition of optical waves and microwaves is satisfied. The group velocity of microwaves can be flexibly designed, and the electric field of microwaves at the band edge

of dispersion can be enhanced and limited in sub-wavelength scale due to the characteristic of slow-light effects, which significantly increases the electro-optic overlap volume and mutual coupling strength. Subsequently, the slow-light effect structure allows a significant reduction in device length, which is of great importance for achieving high modulation efficiency and more compact photonic chips. The design concept of spoof surface plasmonic polaritons structure in this paper can be applied to not only thin-film lithium niobate photonic chips but also other material platforms with high electro-optic coefficients in the future. It also provides a new direction for the development of miniaturized integrated chips from the physical principles of optics and is expected to achieve more complex and diverse photonic circuits integrated with other functional devices.

Key words optical devices; electro-optic modulators; spoof surface plasmon polaritons; slow-light effect; thin-film lithium niobate